Spatial and velocity statistics of inertial particles in turbulent flows

Journal of Physics: Conference Series **333** (2011) 012003 doi:10.1088/1742-6596/333/1/012003

Spatial and velocity statistics of inertial particles in turbulent flows

J. Bec[1], L. Biferale[2,5], M. Cencini[3], A.S. Lanotte[4], F. Toschi[5,6]

[1]Université de Nice-Sophia Antipolis, CNRS, OCA, Lab. Cassiopée, B.P. 4229, 06300 Nice, France

[2]Dept. Physics and INFN, University of Rome "Tor Vergata", Via della Ricerca Scientifica 1, 00133 Rome, Italy

[3]CNR-ISC, Via dei Taurini 19, 00185 Rome, Italy

[4]CNR-ISAC & INFN-Sez. di Lecce, Str. Prov. Lecce-Monteroni, 73100 Lecce, Italy

[5]Department of Physics Eindhoven University of Technology, 5600 MB Eindhoven, The Netherlands

[6]Department of Mathematics and Computer Science, Eindhoven University of Technology, 5600 MB Eindhoven, The Netherlands and CNR-IAC, Via dei Taurini 19, 00185 Rome, Italy

Abstract. Spatial and velocity statistics of heavy point-like particles in incompressible, homogeneous, and isotropic three-dimensional turbulence is studied by means of direct numerical simulations at two values of the Taylor-scale Reynolds number $Re_\lambda \sim 200$ and $Re_\lambda \sim 400$, corresponding to resolutions of 512^3 and 2048^3 grid points, respectively. Particles Stokes number values range from $St \approx 0.2$ to 70. Stationary small-scale particle distribution is shown to display a singular –multifractal– measure, characterized by a set of generalized fractal dimensions with a strong sensitivity on the Stokes number and a possible, small Reynolds number dependency. Velocity increments between two inertial particles depend on the relative weight between smooth events - where particle velocity is approximately the same of the fluid velocity-, and *caustic* contributions - when two close particles have very different velocities. The latter events lead to a non-differentiable small-scale behaviour for the relative velocity. The relative weight of these two contributions changes at varying the importance of inertia. We show that moments of the velocity difference display a quasi bi-fractal-behavior and that the scaling properties of velocity increments for not too small Stokes number are in good agreement with a recent theoretical prediction made by K. Gustavsson and B. Mehlig *arXiv:1012.1789v1 [physics.flu-dyn]*, connecting the saturation of velocity scaling exponents with the fractal dimension of particle clustering.

1. Introduction

Particle suspensions of dust, droplets, or bubbles advected by incompressible turbulent flows are commonly encountered in many natural phenomena (see e.g. [1–6]). The problem is more complicated than in the case of fluid tracers, i.e. small particles with the same density as the carrier fluid. Suspended particles with a finite size and/or a density ratio different from that of the fluid do not follow exactly the flow because of inertial forces. As a consequence, it is crucial to understand the correlations between particle positions and structures of the underlying flow. For instance, heavy/light particles are expelled/attracted from/into vortical structures, a phenomenum that can be exploited to evaluate temporal properties of coherent turbulent structures [7]. As a result, particle *preferentially concentrate* in specific regions of the flow, and

	N	Re_λ	η	δx	ε	ν	τ_η	$t_{\rm dump}$	δt	T_L
Run I	512	185	0.01	0.012	0.9	0.002	0.047	0.004	0.0004	2.2
Run II	2048	400	0.0026	0.003	0.88	0.00035	0.02	0.00115	0.000115	2.2

Table 1. Eulerian parameters for the Runs analysed here: Run I and Run II in the text. N is the number of grid points in each spatial direction; Re_λ is the Taylor-scale Reynolds number; η is the Kolmogorov dissipative scale; $\delta x = \mathcal{L}/N$ is the grid spacing, with $\mathcal{L} = 2\pi$ denoting the physical size of the numerical domain; $\tau_\eta = (\nu/\varepsilon)^{1/2}$ is the Kolmogorov dissipative time scale; ε is the average rate of energy injection; ν is the kinematic viscosity; $\tau_{\rm dump}$ is the time interval between two successive dumps along particle trajectories; δt is the time step; $T_L = L/U_0$ is the eddy turnover time at the integral scale $L = \pi$, and U_0 is the typical large-scale velocity. Stokes number available from the two simulations are: Run I:(0; 0.16; 0.27; 0.37; 0.48; 0.59; 0.69; 0.80; 0.91; 1.01; 1.12; 1.34; 1.60; 2.03; 2.67; 3.31). Run II: (0.0; 0.16; 0.6; 1.0; 3.0; 5.0; 10; 20; 30; 40; 50; 70)

strong inhomogeneities in the particle spatial distribution develop, depending on the relative importance between inertial forces and turbulent advection.

Recent theoretical [8–10]) and numerical [11–14] work have focused on these aspects. Advances in the understanding of the statistical characterization of small particle aggregates have been obtained by studying heavy particles advected by stochastic flows [15–18], and/or in two-dimensional turbulent flows [19]. Temporal properties along single trajectory have been addressed both numerically and experimentally for small, heavy particles and light particles (see, e.g., [20–28]), and for large particles, where inertial effects combine with finite size ones (see e.g. [29–31]).

In our simulations, particles are organised in different families according to the values of their *Stokes number*, St. The Stokes number is defined as $St = \tau_s/\tau_\eta$, i.e. the ratio between the particle response time τ_s and the flow Kolmogorov timescale $\tau_\eta = (\nu/\varepsilon)^{1/2}$, where ν is the flow kinematic viscosity and ε the average rate of energy injection. The response time $\tau_s = 2a^2\rho_f/(9\nu\rho_p)$ depends on the particle radius a, which is assumed to be much smaller than the Kolmogorov scale η, and the ratio between the fluid ρ_f and particle density ρ_p.

In this paper we present a new data analysis concerning a series of high-resolution Direct Numerical Simulations (DNS). In particular, we intend to discuss (i) non-homogeneous effects in the particle spatial distribution, characterized by the whole set of generalized fractal dimensions $D_q(St)$ at changing both the order of the moment q and the Stokes number St; (ii) the connection between scaling properties of high-order moments of particle-particle relative velocity increments and the (multi)fractal spatial properties. Concerning the latter point, we show that our numerical results agree with a recent theoretical prediction [32], at least for not too small Stokes numbers.

2. Equation of motion and numerical details

We present results from a $3D$ DNS of a turbulent flows seeded with inertial particles. The flow phase is described by the Navier-Stokes equations for the velocity field $\boldsymbol{u}(\boldsymbol{x}, t)$

$$\partial_t \boldsymbol{u} + \boldsymbol{u}\cdot\boldsymbol{\nabla}\boldsymbol{u} = -\frac{1}{\rho_f}\boldsymbol{\nabla} p + \nu\Delta\boldsymbol{u} + \boldsymbol{f}, \quad \boldsymbol{\nabla}\cdot\boldsymbol{u} = 0\,. \tag{1}$$

The statistically homogeneous and isotropic external forcing $\boldsymbol{f}$ injects energy in the first low wave number shells, by keeping constant their spectral content [33]. Kinematic viscosity is chosen such that the Kolmogorov length scale $\eta \approx \delta x$, where δx is the grid spacing: this choice

ensures that small-scale velocity dynamics is well resolved. The numerical domain is cubic and 2π-periodic in the three directions of space. We use a fully dealiased pseudospectral algorithm with 2nd order Adam-Bashforth time-stepping (for details see [20, 21]). We performed two series of DNS: Run I with numerical resolution of 512^3 grid points, and the Reynolds number at the Taylor scale $Re_\lambda \approx 200$; Run II with 2048^3 resolution and $Re_\lambda \approx 400$. Details of the runs can be found in Table 1.

The dispersed phase is constituted by millions of heavy particles, with different Stokes number values. Particle sizes are assumed to be much smaller than the Kolmogorov scale of the flow and with a negligible Reynolds number relative to the particle size. These assumptions allow us to consider point particles which evolve according to the dynamics

$$\dot{\boldsymbol{X}} = \boldsymbol{V} , \qquad \dot{\boldsymbol{V}} = -\frac{1}{\tau_s}\left[\boldsymbol{V} - \boldsymbol{u}(\boldsymbol{X}, t)\right] , \tag{2}$$

where the dots denote time derivatives. The particle position and velocity are $(\boldsymbol{X}(t), \boldsymbol{V}(t))$, respectively, while $\boldsymbol{u}(\boldsymbol{X}(t), t)$ is the Eulerian fluid velocity evaluated at the particle position.

Equation (2) has been derived under the assumption of very dilute suspensions, where particle-particle interactions (collisions) and hydrodynamic coupling to the flow can be neglected (see Ref.[34] for a discussion of the complete equation of motion of a small, spherical particle in a non-uniform flow).

For each Stokes number we follow 7×10^6 (Run I) and 10^8 (Run II) particles, for 5 and 2 large-scale eddy-turnover times, respectively. Particles are injected uniformly in the box with initial velocity equal to that of the fluid, and measurements are started only after a steady state statistics is reached (see, e.g., Ref.[21] for details).

3. Mass Distribution

Preferential concentration is responsible for a highly non trivial spatial distribution of particles at changing inertia. Due to its connection with collision kernels, much work has been done to measure and characterize the two-point particle-particle distribution, i.e. the probability to find a pair of particles at a distance $r \ll \eta$, in an ensemble of inertial particle in homogeneous turbulence [11, 13]. The dissipative dynamics of particles is responsible for the convergence of their trajectories towards a dynamically evolving attractor in the position-velocity phase space. As a consequence, the probability density function (PDF) of the inter-particle distances behaves at scales smaller than the Kolmogorov dissipative scale η, as a power law, i.e. $p_2(r) \sim r^{D_2(St)-1}$, where the exponent $D_2(St)$ is usually called the *correlation dimension*. In general, there is no reason to expect a complete statistical self-similarity of the mass distribution, which would give equal generalized dimension $D_q(St)$ for any order q. Thus the full characterization of the particle density field requires the knowledge of the full spectrum of generalized dimensions. This has already been argued theoretically and found numerically for the case of paticles in random flows and/or smooth flows [35, 36]. We present here the first measurements of the generalized fractal dimensions $D_q(St)$ as a function of the Stokes number and give some insight on the large mass fluctuations.

The formal definition of generalized dimensions generally relies on box-counting techniques. For that, let us cover at a fixed time t, for each given St, the particle set with $N_r(St)$ balls of size r. We define the instantaneous local mass distribution $m_r(\boldsymbol{x}_i, t)$ inside the ith ball centered at $\boldsymbol{x}_i$ as the fraction of particles inside this ball. Then, one can fully characterize the particle distribution by studying the behaviour of the moments of order q of m_r at changing the ball radius, r. By definition of Hausdorff dimension we have that $\langle N_r(St)\rangle \sim r^{-D_0(St)}$, where $\langle\cdot\rangle$ denote ensemble averages (equivalent to time averages when ergodicity is assumed). The whole spatial particle distribution can then be characterized by the behaviours of the moments of m_r

for different orders:

$$M_r^{(q)}(St) = \left\langle \sum_{i=1}^{N_r(St)} m_r^q(\boldsymbol{x}_i, t) \right\rangle = \left\langle \overline{m_r^{q-1}} \right\rangle, \tag{3}$$

where the over-bar average is a Lagrangian average; it is made on the attractor so that it is locally weighted with the mass of particles itself. For a multifractal distribution we expect for $r \ll \eta$:

$$M_r^{(q)}(St) \sim r^{(q-1)D_q(St)}. \tag{4}$$

The generalized dimensions $D_q(St)$ fully determines the spatial mass distribution for each Stokes number.

In the stationary regime, for almost all balls centered on the attractor, the local dimension $h = \ln m_r / \ln r$ tend to a time-constant, deterministic value $D_1(St)$, which is usually called the *information dimension*. For finite length scales r, the fluctuations with respect to $D_1(St)$ of the local dimension h on the attractor are described by a large-deviation principle, which implies that they take the form $\overline{p}_r(h; St) \propto r^{f(h;St)}$, where the density probability $\overline{p}_r$ is evaluated on balls centered on the attractor. The function $f(h)$ is generally called the multifractal (or singularity) spectrum. The generalized dimensions are related to it via

$$(q-1)\, D_q(St) = \inf_h \left[(q-1)\, h + f(h; St) \right]. \tag{5}$$

Note that if the particles were to be distributed with a spatial density $\rho(\boldsymbol{x}, t)$, the coarse-grained mass would simply read

$$m_r(\boldsymbol{x}_i, t) = \int_{|\boldsymbol{y}|<r} d\boldsymbol{y}\, \rho(\boldsymbol{x}_i + \boldsymbol{y}, t), \tag{6}$$

so that its moment of order q would relate to the integral over balls of size r of the q-th order correlator of the density:

$$M_r^{(q)}(St) = \int_{|\boldsymbol{y}_2|<r} \dots \int_{|\boldsymbol{y}_q|<r} d\boldsymbol{y}_2 \cdots d\boldsymbol{y}_q\, \langle \rho(0,t)\rho(\boldsymbol{y}_2,t) \cdots \rho(\boldsymbol{y}_q,t) \rangle. \tag{7}$$

A measurement and evaluation of the generalized fractal dimensions that is based on one of their properties described above requires having a good small-scale approximation of the mass distribution. This is generally not the case in numerical simulations since the finite number of particles is responsible for very strong effects of discreteness at small scales.
In order to cope with this difficulty, it is much easier to deal with the q-point particle distribution. The probability $P_q(r; St)$ to observe q particles randomly chosen on the attractor, all lying within a distance r, behaves at small scales as $P_q(r; St) \propto r^{(q-1)D_q(St)}$. For the case $q = 2$, one indeed gets $\mathrm{d}P_2(r)/\mathrm{d}r = p_2(r) \propto r^{D_2(St)-1}$. We made use of this technique based on the q-point cumulative probabilities P_q in order to evaluate the fractal dimensions of inertial particles in our numerical simulations.

Figure 1 (left) represents the generalized fractal dimensions as a function of Stokes from Run I. The statistics shows a clear signature of multifractality, confirming the results already obtained in random flows [36]. A straightforward method for evaluating the scaling properties of $P_q(r)$ is to look at the behavior of its logarithmic derivative $(\mathrm{d}\ln P_q(r))/(\mathrm{d}\ln r)$. Such a quantity defines a local slope, which tends to $(q-1)D_q$ as $r/\eta \to 0$. To extract a scaling exponent, a choice is to average this local slope over an interval where it is reasonably constant; error bars can then be defined as maximal deviations of the actual local slope from this average. Following such procedure error bars may become large, order %10 for the highest moment shown in the left panel of Fig. (1). Here we made use of a different strategy. As seen from the right panel of Fig. 1,

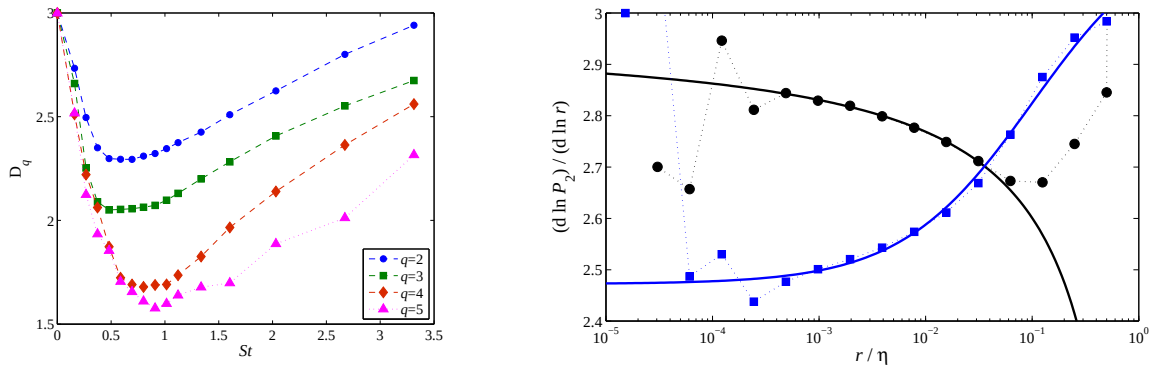

Figure 1. Left: generalized fractal dimensions $D_q(St)$ measured from Run I, as a function of the Stokes number for moment of order $q = 2$ to $q = 5$. Results from Run II do not show any significative dependency (not shown). Right: local slope of the two-point cumulative probability $P_2(r; St)$ as a function of scale for two different values of the Stokes number (lower blue: $St = 0.48$ and upper black: $St = 3.31$); the two solid lines represent the fit obtained from accounting for expected subleading terms.

there is no clear scaling range larger than a fraction of a decade where the local slope observed from our numerical data is decently constant. However, there is a sufficient statistical accuracy for resolving a smooth behaviour of the local slope over more than two decades. Making use of this requires accounting for subleading terms and thus formulating the following Ansatz for the small-scale behaviour of $P_q(r)$:

$$P_q(r) \approx r^{(q-1)D'_q} \left[\alpha_0 + \alpha_1 r + \alpha_2 r^2 + \cdots\right] + r^{3(q-1)} \left[\beta_0 + \beta_1 r + \beta_2 r^2 + \cdots\right], \tag{8}$$

The decomposition in two separate contributions follows from [37]. The first term involves the phase-space dimension D'_q, which describes the particle distribution in the full position-velocity space. The second term comes from the projection of this set onto the position space and relates to the development of caustics (i.e. of spatial locations with more than one particle velocity that become singular upon projection). This Ansatz suggests that $D_q = \min(D'_q, 3)$. The form of the first-order subleading term at a given scale r strongly depends on the values of the coefficients α_i and β_i. At small values of the Stokes number, $D'_q < 3$ and the β_i's are very close to 0. This relates the particle clustering properties, and to a very small probability to observe caustics, which is expected to be of the form $\propto \exp(-c/St)$ (see [38] and next section). At larger Stokes numbers, the caustics give the main subleading contribution.
Hence, two different possible fits for the q-point probability can be considered

$$P_q(r) \approx \alpha_0\, r^{(q-1)D'_q} + \alpha_1\, r^{(q-1)D'_q+1} \quad \text{for } St \le St_\star, \tag{9}$$

$$P_q(r) \approx \alpha_0\, r^{(q-1)D'_q} + \beta_0\, r^{3(q-1)} \quad \text{for } St \ge St_\star, \tag{10}$$

where $St_\star$ approximately corresponds to the value of the Stokes number where the minimum of the dimension D_q is attained, and small-scale clustering is maximal. When applied to the logarithmic derivative, such forms allow one to fit the data with two parameters (D'_q and the ratio of the two constants) over more than two decades, as seen from Fig. 1 (right).

The measurement of fractal dimensions obtained from this technique are shown on Fig. 1 (left). They show two very different behaviours at very small and moderate Stokes. On the left-hand side of the minimum, the dimensions D_q seem to saturate very quickly to a fixed limit

D_∞ when q increases. The saturation is much slower at larger values of the Stokes number. This suggests that, eventhough two particle sets with different Stokes numbers located below and above $St_\star$ can display the same correlation dimension D_2, the fluctuations of their mass at the same scale will be of very different nature. Such a consideration, which still requires to be understood in a quantitative way, might be very important when evaluating instantaneous collision rates between heavy particles.

4. Statistical Properties of the Relative Velocity

In this section, we discuss the statistics of the relative velocity between heavy particle pairs, having the same Stokes number, conditioned on their separation. This is an important subject relevant to the build up of models for particle collisions [3, 17, 39]. We define the relative velocity between a particle pair as

$$\delta_R V_{St}(t) \;=\; |\boldsymbol{V}_1(\boldsymbol{X}_1(t),t) - \boldsymbol{V}_2(\boldsymbol{X}_2(t),t)|, \tag{11}$$

with $R = |\boldsymbol{X}_1 - \boldsymbol{X}_2|$, the pair distance vector. The statistical properties of $\delta_R V_{St}$ can be characterized in terms of the conditional moments

$$S_p(r;St) = \langle\, |\delta_R V_{St}|^p \;|\; R{=}r \rangle\,. \tag{12}$$

Since we work in stationarity conditions, with an homogeneous and isotropic velocity field, the dependence of S_p on time, space and direction of $\boldsymbol{R}$ drops out. In the following, we will discuss the scaling behaviour of moments of relative velocity at varying the degree of inertia and the distance between the particles.

The qualitative behavior of $\delta_R V_{St}$ can be readily understood as follows. If the particle response time τ_s is much smaller than the characteristic time $\tau(R)$ of fluid velocity fluctuations on scale R, particle velocities will be very close to fluid velocities at particle position so that $\delta_R V(St) \approx \delta_R u$. On the other hand, if the particle response time is larger than $\tau(R)$, particle velocities will be uncorrelated with the fluid and among each other, thus one expects that $\delta_R V(St) \approx const.$ This leads to introduce the notion of scale dependent Stokes number [40–42] $St(r) = \tau_s/\tau(R)$, where $\tau(R) \approx \epsilon^{-1/3} R^{2/3}$ if $R > \eta$, i.e. for inertial range scales, and $\tau(R) = \tau_\eta$ for $R \leq \eta$, i.e. for scales belonging to the dissipative range.
Hence, for what concerns the statistics of relative velocity, at a given scale R particle inertia is small or large depending on $St(R)$. In Fig. 2, we observe that such a qualitative behavior is well reproduced by the second order structure function $S_2(r, St)$, as a function of the scale and for different values of $St = \tau_s/\tau_\eta$. For larger scales, $S_2(r, St)$ tends to recover the fluid behavior characterized by a Kolmogorov like $r^{2/3}$ scaling [42]. For larger Stokes values, the scale R at which the fluid velocities are recovered becomes larger (see Fig.5 in [43]). However, at scales within the dissipative range, we observe a strong dependence of $S_2(r;St)$ on the Stokes number suggesting that

$$S_p(r, St) \sim r^{\xi_p(St)} \tag{13}$$

i.e. within the available scale range accessible by our DNS, we observe a scaling behavior with an exponent $\xi_p(St)$ which non-trivially depends both on the order of the statistics and on the Stokes number. it is interesting to discuss such dependency and to connect it with particle statistical dynamics. In Figure 3, we show the behavior of the fitted exponent $\xi_p(St)$ at varying both the order p and the Stokes number St [43]. Two features can be readily identified. First we note that, at fixed St, for increasing the order p, the exponent $\xi_p(St)$ changes from a linear dependence on p ($\xi_p(St) = p$) to a p-independent value $\xi_\infty(St)$, showing a tendency to saturation, similarly to what happens in Burgers turbulence [44]. In particular, the scaling exponents are rather well approximated by a bi-fractal behavior:

$$\xi_p(St) = \min\{p, \xi_\infty(St)\}\,. \tag{14}$$

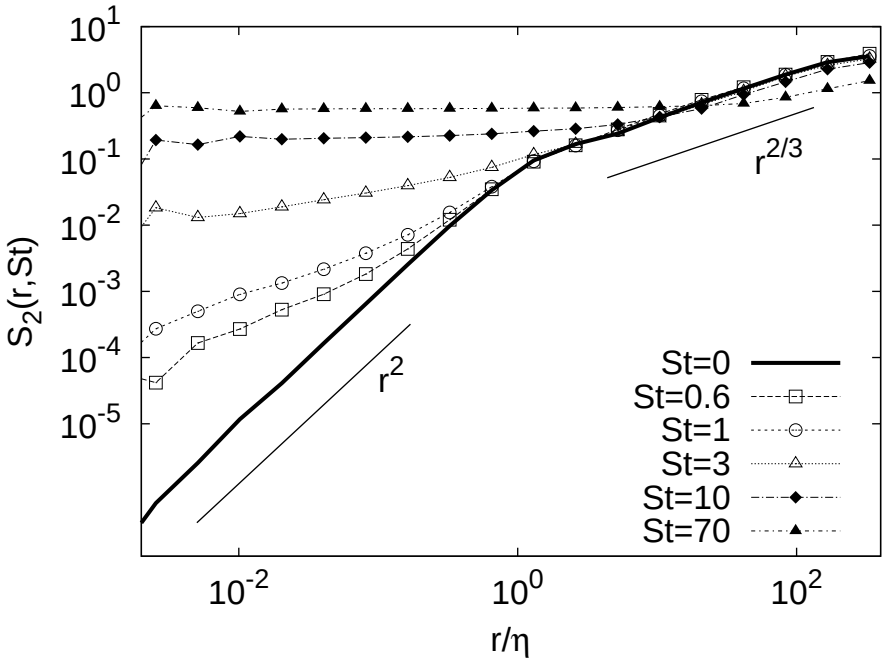

Figure 2. Log-log plot of the second order moment of the conditional velocity difference $S_2(r;St)$, as a function of r/η for Run II (from [42]).

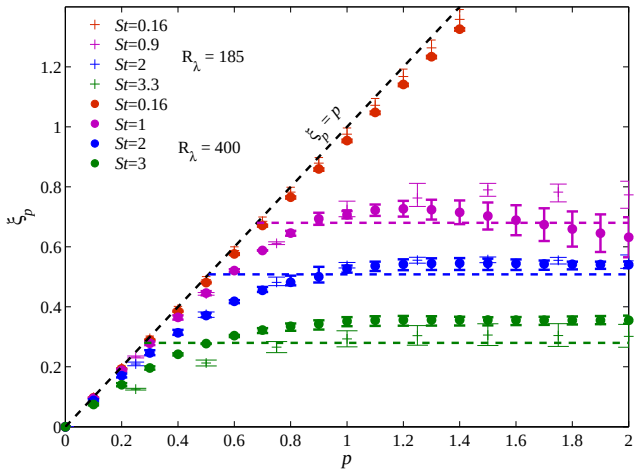

Figure 3. The scaling exponents ξ_p vs the order p, for different Stokes numbers and for both Runs (see also [43]).

Note that to disentangle a *pure* bi-fractal behavior from a multifractal one in presence of a saturation of scaling exponents is not simple, and requires a statistical convergence not easily achievable for 3D flows. However, as discussed below, there are good reasons to favor the former type of scaling behavior.

Second we note that the saturation exponent $\xi_\infty(St)$ dramatically depends on St. In particular, it decreases from values larger than 1, for $St < 1$, to values smaller and smaller at increasing St. Data suggest that $\xi_\infty(St) \approx 0$ when St reaches values $\approx 7 - 8$. Therefore, velocity increments

become rougher as St increases, departing more and more from the smooth differentiable behaviour.

These observations can be interpreted in terms of *caustic* contributions [38, 45], or *sling effect* [3, 10]. The physical observation is that, due to inertia, relative velocity differences $\delta_R V_{St}$ may not go smoothly to zero when the particle separations decreases. Indeed, particle dynamics in phase space is dissipative and the set where particle trajectories evolve may fold in the velocity direction leading to the formation of such caustics [17]. This effect becomes dramatic when inertia is such that particle response time is larger than any turbulent flow time scale: in such case, nearby particles will move with uncorrelated velocities [37, 46], and caustics are dense in space. The statistical importance of caustics does change with the Stokes number.

Recently, theoretical arguments have been put forward about the scaling behaviour for conditioned structure functions $S_p(r; St)$ in the dissipative range of the 3D turbulence, based on results obtained in stochastic flows [32, 47]. In particular, for scales $r/\eta \to 0$, it is expected that,

$$S_p(r; St) \sim A_p(St)(r/\eta)^p + B_p(St)(r/\eta)^{3-D_2(St)} \,. \tag{15}$$

The first term in (15) corresponds to the smooth (differentiable) part of the particles' velocity distribution where $A_p(St)$ is a $O(1)$ constant. The second term represents the contribution from caustics. Notice that the exponent $D_2(St)$ is the correlation dimension of the set in position space where particles concentrate (see previous section). The above prediction was obtained by solving in the limit $r \to 0$, the equation that rules the joint probability to find a particle pair at separation $R = r$ with a relative velocity $\delta_R V_{St}$. Such equation can be solved for a one dimensional stochastic flow. Extending the same ideas to flows in two and three dimensions, one gets to (15) as shown recently in [32]. In equation 15, the constant in front of the caustic contribution is suggested to be

$$B_p(St) \sim \exp(-C_p/St) \,, \tag{16}$$

and it is related to the rate at which caustics are formed [38, 48]. Note that while $A_p(St)$ is an $O(1)$ constant, possibly dependent on St, the activation factor B_p goes extremely fast at zero when $St \to 0$.

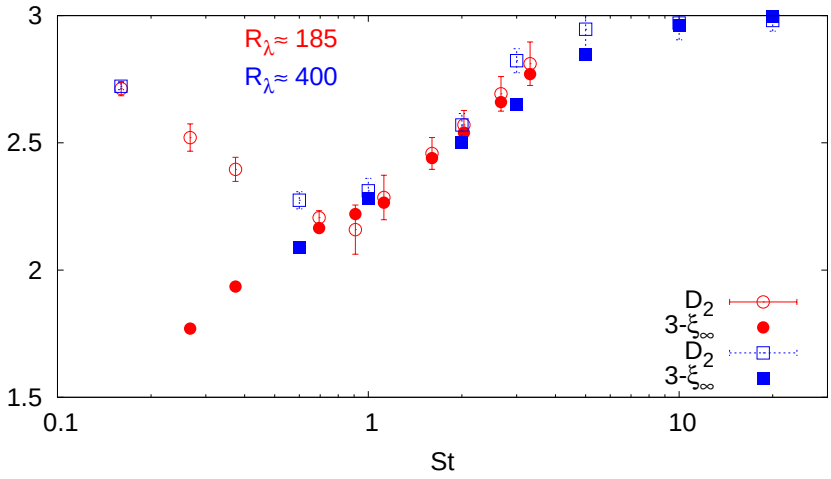

Figure 4. Comparison of the exponents $D_2(St)$ and $3 - \xi_\infty(St)$ vs St for Run I (red data, circles) and Run II (blue data, squares).

From equation (15) a simple bi-fractal behaviour is predicted for asymptotically small

distances i.e., $S_p(r, St) \sim r^{\xi_p(St)}$ with

$$\xi_p(St) = \min\{p, 3 - D_2(St)\}. \tag{17}$$

Comparing eq. (17) with eq. (14), obtained on the basis of the observed behavior (Fig. 3), we get a prediction for the saturation exponent

$$\xi_\infty(St) = 3 - D_2(St)\,, \tag{18}$$

that can be checked with the DNS data. Figure 4 shows in the same plot $D_2(St)$ and $3-\xi_\infty(St)$ as measured in both Runs.
For Stokes numbers larger than that for which $D_2(St)$ is minimal ($St \simeq 0.7$), the prediction (18) is rather well verified by our numerical data. While for smaller Stokes values, a discrepancy is observed between the value od the correlation dimension and the saturation exponent.

Two different comments can be made. By matching the statistical weigh of the two terms in (15), we observe that the asymptotic regime is expected only for scales $r < r_c(p, St) \sim B_p(St)^{1/(p-3+D_2)}$, which become exponentially small when $St \sim 0$. In our numerics, the range of scales allowing to fit the scaling properties is limited to an interval $[r_{min}, \eta]$. Clearly, the bifractal behavior (17) can be observed only if $r_{min} \ll r_c(p, St)$, otherwise only the smooth scaling would be observed $\xi_p(St) = p$. Hence, in general, it may be very difficult to test the prediction (18) for small Stokes number. On the other hand, we notice that for small Stokes values our data do not suggest a pure smooth scaling $\xi_p(St) = p$, but are compatible with a saturation of high order scaling exponents ξ_p to a value different from that predicted by eq. (18). In conclusion, it is fair to say that while for $St > 1$ the picture derived from (15) works rather well, for $St \ll 1$ there is still some difficulty to validate it. Either the saturation we observe is the result of some spurious effect due to the limited range of avalaible scales, or there is still something to understand in the limit of very small inertia.

5. Conclusions

We studied the spatial and velocity statistics of point-like heavy particles in stationary, incompressible, homogeneous and isotropic three-dimensional turbulence at two values of the Reynolds number, $Re_\lambda \sim 200$ and $Re_\lambda \sim 400$. We considered the behavior of tracers ($St = 0$), and heavy particles with Stokes number from $St = 0.16$ to 70.
Stationary small-scale particle distribution display a singular –multifractal– measure, characterized by a set of generalized fractal dimensions with a strong sensitivity on the Stokes number and a small –if any– Reynolds number dependency. Velocity increments between a pair of particles conditioned to be at a given distance depend on the relative weight of *smooth* events, where the particle velocity difference is approximately the equal to the fluid velocity difference, and *caustics* contributions, i.e. associted to close particles having very different velocities. The latter events lead to a non-differentiable small-scale behaviour for the relative velocity. The relative weight of these two mechanisms changes at varying Stokes number. We showed that moments of the velocity difference enjoy a quasi bi-fractal-behavior, and that the scaling properties of velocity increments for not too small Stokes numbers are in good agreement with a recent theoretical prediction made by K. Gustavsson and B. Mehlig [32].

ACKNOWLEDGEMENTS. This study benefited from fruitful discussions with G. Falkovich, B. Mehlig, and M. Wilkinson. JB and AL acknowledge support from NSF under grant No. PHY05 51164 for their stay at the Kavli Institute for Theoretical Physics in the framework of the 2008 Physics of Climate Change program. Part of this work was supported by ANR under grant No. BLAN07-1 192604. Simulations were performed at CASPUR and CINECA (Italy), and in the

framework of the DEISA Extreme Computing Initiative supported by the DEISA Consortium (co-funded by the EU, FP6 project 508830).

References

[1] Csanady, G. 1980 *Turbulent diffusion in the environment.* Geophysics and Astrophysics Monographs Vol. 3 D. Reidel Publishing Company.
[2] Eaton, J.K.& Fessler, J.L. 1994 Preferential concentrations of particles by turbulence. *Intl. J. Multiphase Flow* **20**, 169–209.
[3] Falkovich, G., Fouxon, A. & Stepanov, M. 2002 Acceleration of rain initiation by cloud turbulence. *Nature* **419**, 151–154.
[4] Post, S. & Abraham, J. 2002 Modeling the outcome of drop-drop collisions in Diesel sprays. *Intl. J. Multiphase Flow* **28**, 997–1019.
[5] Shaw, R.A. 2003 Particle-turbulence interactions in atmospheric clouds. *Ann. Rev. Fluid Mech.* **35**, 183–227.
[6] Toschi, F. & Bodenschatz, E. 2009 Lagrangian Properties of Particles in Turbulence. *Ann. Rev. Fluid Mech.* **41**, 375–404 .
[7] Biferale, L., Scagliarini, A. & Toschi, F. 2010 On the measurement of vortex filament lifetime statistics in turbulence. *Phys Fluids* **22** 065101.
[8] Balkovsky, E., Falkovich, G. & Fouxon, A. 2001 Intermittent distribution of inertial particles in turbulent flows. *Phys. Rev. Lett.* **86**, 2790–2793.
[9] Zaichik, L.I., Simonin, O. & Alipchenkov, V.M. 2003 Two statistical models for predicting collision rates of inertial particles in homogeneous isotropic turbulence. *Phys. Fluids* **15**, 2995–3005.
[10] Falkovich, G. & Pumir, A. 2004 Intermittent distribution of heavy particles in a turbulent flow. *Phys. Fluids* **16**, L47–L51.
[11] Collins, L.R. & Keswani, A. 2004 Reynolds number scaling of particle clustering in turbulent aerosols. *New J. Phys.* **6**, 119.
[12] Chun, J., Koch, D.L., Rani, S., Ahluwalia, A. & Collins, L.R. 2005 Clustering of aerosol particles in isotropic turbulence. *J. Fluid Mech.* **536**, 219–251.
[13] Bec, J., Biferale, L., Boffetta, G., Cencini, M., Lanotte, A.S., Musacchio, S. & Toschi, F. 2007 Heavy particle concentration in turbulence at dissipative and inertial scales. *Phys. Rev. Lett.* **98**, 084502.
[14] Goto, S. & Vassilicos, J.C. 2008 Sweep-stick mechanism of heavy particle clustering in fluid turbulence. *Phys. Rev. Lett.* **100** 054503.
[15] Sigurgeirsson H. & Stuart A.M. 2002 A Model for Preferential Concentration. *Phys. Fluids* **14**, 4352–4361.
[16] Mehlig, B. & Wikinson, M. 2004 Coagulation by random velocity fields as a Kramers problem. *Phys. Rev. Lett.* **92**, 250602.
[17] Bec, J., Celani, A., Cencini, M. & Musacchio, S. 2005 Clustering and collisions of heavy particles in random smooth flows. *Phys. Fluids* **17**, 073301.
[18] Olla, P. 2002 Transport properties of heavy particles in high Reynolds number turbulence. *Phys. Fluids* **14**, 4266–4277.
[19] Boffetta, G., De Lillo, F. & Gamba, A. 2004 Large scale inhomogeneity of inertial particles in turbulent flows. *Phys. Fluids* **16**, L20–L24.
[20] Bec, J., Biferale, L., Boffetta, G., Celani, A., Cencini, M., Lanotte, A.S., Musacchio, S., & Toschi, F. 2006 Acceleration statistics of heavy particles in turbulence. *J. Fluid Mech.* **550**, 349–358.
[21] Cencini, M., Bec, J., Biferale, L., Boffetta, G., Celani, A., Lanotte, A.S., Musacchio, S. & Toschi, F. 2006 Dynamics and statistics of heavy particles in turbulent flows. *J. Turb.* **7**, 36, 1.
[22] Gylfason, A., Ayyalasomayajula, S., Bodenschatz, E. & Warhaft, Z. 2006 Lagrangian measurements of inertial particle accelerations in grid generated wind tunnel turbulence. *Phys. Rev. Lett* **97**, 144507.
[23] Gerashchenko, S., Sharp, N.S., Neuscamman, S. & Warhaft, Z. 2008 Lagrangian measurements of inertial particle accelerations in a turbulent boundary layer. *J. Fluid Mech.* **617**, 255–281.
[24] Zaichik, L.I. & Alipchenkov, V.M. 2008 Acceleration of heavy particles in isotropic turbulence. *Intl. J. Multiphase Flow* **34**, 865–868.
[25] Ayyalasomayajula, S., Warhaft, Z. & Collins, L.R. 2008 Modeling inertial particle acceleration statistics in isotropic turbulence. *Phys. Fluids* **20** 095104.
[26] Volk, R., Mordant, N., Verhille, G. & Pinton, J.-F. 2008 Laser Doppler measurement of inertial particle and bubble accelerations in turbulence, *Europhys. Lett* **81**, 34002.
[27] Volk, R., Calzavarini, E.,Verhille, G., Lohse, D., Mordant, N., Pinton, J.-F. & Toschi, F. 2009 Acceleration of heavy and light particles in turbulence: comparison between experiments and direct

numerical simulations, *Phys. D* in press.
[28] Benzi, R., Biferale, L., Calzavarini, E., Lohse, D. & Toschi, F. 2009. Velocity gradients statistics along particle trajectories in turbulent flows: the refined similarity hypothesis in the Lagrangian frame. *Phys. Rev. E* **80**, 066318.
[29] Qureshi, N.M., Bourgoin, M., Baudet, C., Cartellier, A., & Gagne, Y., 2007 Turbulent transport of material particles: An experimental study of finite size effects. *Phys. Rev. Lett* **99**, 184502.
[30] Xu H. & Bodenschatz E. 2008 Motion of inertial particles with size larger than Kolmogorov scale in turbulent flows. *Physica* D **237**, 2095–2100.
[31] Qureshi, N.M., Arrieta, U., Baudet, C., Cartellier, A., Gagne, Y. & Bourgoin, M. 2008 Acceleration statistics of inertial particles in turbulent flow. *Eur. Phys. J. B* **66**, 531–536.
[32] Gustavsson, K. & Mehlig, B. 2010. Distribution of relative velocities in turbulent aerosols. arXiv:1012.1789.
[33] Chen, S., Doolen, G.D., Kraichnan, R.H. & She, Z.-S. 1993 On statistical correlations between velocity increments and locally averaged dissipation in homogeneous turbulence. *Phys. Fluids A* **5**, 458–463.
[34] Maxey, M.R. & Riley, J. 1983 Equation of motion of a small rigid sphere in a nonuniform flow. *Phys. Fluids* **26**, 883–889.
[35] Bec, J. 2003 Fractal clustering of inertial particles in random flows *Phys. Fluids* **15**, L81–L84.
[36] Bec, J., Gawedzki, K. & Horvai, P. 2004. Multifractal clustering in compressible flows. *Phys. Rev. Lett.* **92**, 224501.
[37] Bec, J., Cencini, M. & Hillerbrand, R. 2007 Heavy particles in incompressible flows: the large Stokes number asymptotics. *Physica* D **226**, 11–22.
[38] Wilkinson M. & Mehlig B. 2005 Caustics in turbulent aerosols. *Europhys. Lett* **71**, 186–192.
[39] Wilkinson, M. , Mehlig B., & Bezuglyy, V. 2006. Caustic activation of rain showers. *Phys. Rev. Lett.* **97**, 48501.
[40] Falkovich, G. Fouxon, A. & Stepanov, P. 2003 in *Sedimentation and Sediment Transport*, edited by A. Gyr and W. Kinzelbach, Kluwer Academic, Dordrecht, pp. 155-158.
[41] Bec, J., Cencini, M. & Hillerbrand, R. 2007 Clustering of Heavy particles in random self-similar flows . *Phys. Rev. E* **75**, 025301.
[42] Bec, J., Biferale, L., Lanotte, A.S., Toschi, F. & Scagliarini, A. 2010 Turbulent pair dispersion of inertial particles *J. Fluid Mech.* **645** 497.
[43] Bec, J., Biferale, L., Cencini, M., Lanotte, A.S. & Toschi, F. 2010 Intermittency in the velocity of heavy particles in turbulence. *J. Fluid Mech.* **646** 527.
[44] Frisch, U. 1995 *Turbulence. The legacy of A.N. Kolmogorov* Cambridge University Press, Cambridge (UK).
[45] Falkovich, G. & Pumir, A. 2007 Sling effect in collision of water droplet in turbulent clouds. *J. Atm. Sci.* **64**, 4497–4505.
[46] Abrahamson J. 1975 Collision rates of small particles in a vigorously turbulent fluid. Chem. Eng. Sci. **30** 1371–1379.
[47] Cencini, M., Bec, J. 2009 Talk given at working group meeting of COST action MP0806.
[48] Derevyanko, S.A., Falkovich, G., Turitsyn, K. & Turitsyn S. 2007 Lagrangian and Eulerian descriptions of inertial particles in random flows. *J. Turb.* **8**, 16, 1–19.